Available online at www.sciencedirect.com
SCIENCE DIRECT
Electric Power Systems Research 76 (2006) 801–807
ELECTRIC POWER SYSTEMS RESEARCH
www.elsevier.com/locate/epsr

Enhancement of power system dynamic performance through an on-line self-tuning adaptive SVC controller

A.H.M.A. Rahim [a,*], E.P. Nowicki [b], O.P. Malik [b]

[a] *Department of Electrical Engineering, K.F. University of Petroleum & Minerals, Dhahran, Saudi Arabia*
[b] *Department of Electrical & Computer Engineering, University of Calgary, Calgary, AB, Canada*

Accepted 3 July 2005
Available online 27 December 2005

Abstract

Static VAr compensators (SVC) are used for voltage control of long distance bulk power transmission lines. By using a supplemental control loop an SVC can also be used to improve the dynamic and transient stability of a power system. Use of a self-tuning adaptive control algorithm as a supplementary controller for the SVC is presented in this article. The control derived is based on a pole-shifting technique employing a predicted plant model. Simulation studies on a simple power system model showed rapid convergence of the estimated plant parameters with an extremely good damping profile. The controller has been tested for ranges of operating conditions and for various disturbances. The effectiveness of the adaptive damping controller was also evaluated through an 'optimized' PI controller.

Keywords: SVC; Power system damping; Adaptive control; Pole-shift technique; PI control

1. Introduction

Thyristor controlled reactors and capacitors, termed as static VAr compensators (SVC) are applied by utilities in transmission applications for several purposes. The primary purpose is usually rapid control of voltage at weak points in a network [1]. Voltage controlled SVC, as such, does not provide any damping to the power system [2,3]. However, supplemental signals to the voltage set point can be used to improve system damping [4,5].

Control design for the nonlinear power system is often carried out through linearized system models. The methods include exact linearization, linear quadratic regulator theory, direct feedback linearization, etc. Stabilizers based on conventional linear control theory with fixed parameters can be very well tuned to an operating condition and provide excellent damping under that condition, but they cannot provide effective control over a wide operating range for systems that are nonlinear, time varying and subject to uncertainty. It is desirable to develop a controller which has the ability to adjust its own parameters, finding the system structure or model on-line according to the environment in which it works to yield satisfactory control performance. Application of adaptive control theory to excitation control problems is well documented in the literature [6,7]. Adaptive control of SVC systems has been reported in the literature over the number of years. These include adaptive quadratic Gaussian control [8], stabilizer using stochastic variant parameter [9], variable structure adaptive SVC controller [10], etc. Since a precise dynamic model of a power system is difficult to find because of system uncertainties, control design from real-time measurements based on on-line identified models is an attractive alternative.

This article presents an SVC controller design which identifies the model on-line and tunes the parameters of the model adaptively. The control design is carried out through a variable pole-shift method employing the identified system model. Simulation studies indicate that the proposed algorithm converges very rapidly and provides effective damping control. The damping properties are also evaluated through an optimized conventional PI controller.

2. The system configuration

A synchronous generator connected to a large power system over a long transmission line, as shown in Fig. 1, is considered

* Corresponding author. Tel.: +966 3 860 2277; fax: +966 3 860 3535.
E-mail addresses: ahrahim@kfupm.edu.sa (A.H.M.A. Rahim), enowicki@ucalgary.ca (E.P. Nowicki), maliko@ucalgary.ca (O.P. Malik).

0378-7796/$ – see front matter © 2005 Elsevier B.V. All rights reserved.
doi:10.1016/j.epsr.2005.07.006

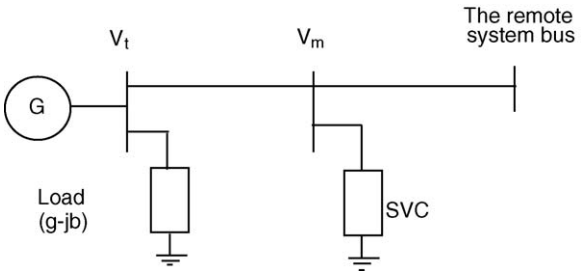

Fig. 1. Power system configuration with SVC.

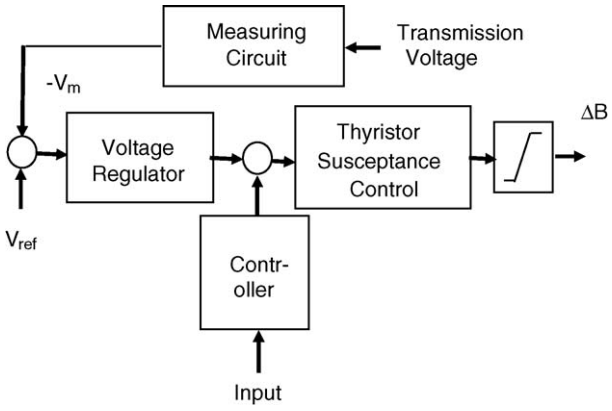

Fig. 2. SVC functional blocks.

for this study. The SVC is placed at the middle of the transmission line which is generally considered to be the ideal site. The generator is assumed to be equipped with an IEEE type-ST excitation system and has a local load connected at its terminal.

Fig. 2 shows a block representation of the SVC system. The SVC is modeled by a susceptance in the same manner as for power flow calculations, but varying within limits depending on the control performed by the voltage regulator of the SVC. A supplementary stabilizer can be connected to the summing junction of the SVC, with feedback signals derived from the system. The voltage at the controlled bus is measured and compared with the reference voltage, which is assumed to be at its rated value. The voltage error is amplified and used to change the susceptance of a reactor unit at the controlling bus.

The plant input (u) in Fig. 3 is the control input to the thyristor firing circuit of the SVC, while the change in generator output (ΔP_e) is the output, y.

3. Self-tuning adaptive regulator

Self-tuning control employs a feedback controller loop in which the controller parameters are modified depending on the error between the real plant output and estimated outputs, as shown in Fig. 3. The control algorithm consists of two stages—a relatively simple linear model of the plants, the parameters of which are estimated and updated regularly, and design the control strategy on the basis of this updated plant model.

The plant model is assumed to be of the form:

$$A(z^{-1})y(t) = B(z^{-1})u(t) + e(t) \tag{1}$$

where $y(t)$, $u(t)$ and $e(t)$ are system output, input and the white noise, respectively; z^{-1} is the delay operator. The polynomial A and B are defined as:

$$A(z^{-1}) = 1 + a_1 z^{-1} + a_2 z^{-2} + a_3 z^{-3} + a_4 z^{-4} + \cdots \tag{2}$$

$$B(z^{-1}) = 1 + b_1 z^{-1} + b_2 z^{-2} + b_3 z^{-3} + b_4 z^{-4} + \cdots \tag{3}$$

The vector of parameters $\theta(t) = [a_1 a_2 \ldots, b_1 b_2 \ldots]^{\mathrm{T}}$ can be calculated recursively on-line through the recursive least square [6] technique as:

$$\theta(t+1) = \theta(t) + K(t)[y(t) - \theta^{\mathrm{T}}(t)\psi(t)] \tag{4}$$

The measurement vector, modifying gain vector and the covariance matrix, respectively are,

$$\begin{aligned} \psi(t) &= [\,-y(t-1) \quad y(t-2)\cdots y(t-n_a) \quad u(t-1)u(t-2)\cdots u(t-n_b)\,]^{\mathrm{T}} \\ K(t) &= \frac{P(t)\psi(t)}{\lambda(t) + \psi^{\mathrm{T}}(t)P(t)\psi(t)} \\ P(t+1) &= \frac{1}{\lambda(t)}[P(t) - K^{\mathrm{T}}(t)P(t)\psi(t)] \end{aligned} \tag{5}$$

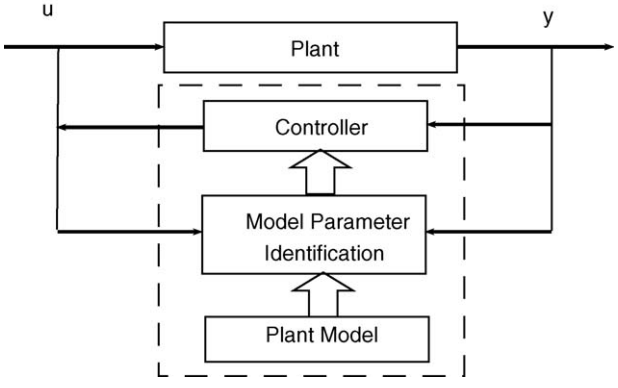

Fig. 3. Block diagram of self-tuning controller.

$\lambda(t)$ is the forgetting factor; n_a and n_b denote the order of the polynomials A and B, respectively. The identified parameters in (4) can be considered as the weighted sum of the previously identified parameters and those derived from the present signals. For systems with constant parameters $\lambda = 1$ produces convergence of the algorithm while for systems with time-varying parameter a variable forgetting factor given by [11],

$$\lambda(t) = \frac{\mathrm{trace}[P(t) - K(t)\psi^{\mathrm{T}}(t)P(t)]}{\mathrm{trace}(P_0)} \tag{6}$$

is required to maintain the trace of the error covariance matrix constant. In the above, P_0 is the initial error covariance matrix and $P(t)$ is the matrix at the iteration before discounted by

λ. Using the forgetting factor, the error covariance matrix is updated at each sampling instant by,

$$P(t) = \frac{P(t-1)}{\lambda(t)} \tag{7}$$

4. The control strategy

Using the parameters obtained from the real time parameter identification method, a self-tuning controller based on pole assignment is computed on-line and fed to the plant. Under the pole-shifting control strategy, the poles of the closed loop system are shifted radially towards the centre of the unit circle in the z-domain by a factor α, which is less than one. The procedure for deriving the pole-shifting algorithm [12] is given below.

Assume that the feedback loop has the form:

$$\frac{u(t)}{y(t)} = -\frac{G(z^{-1})}{F(z^{-1})} \tag{8}$$

where

$$F(z^{-1}) = 1 + f_1 z^{-1} + f_2 z^{-2} + f_3 z^{-3} + f_4 z^{-4} + \cdots + f_{n_f} z^{-n_f}$$

$$G(z^{-1}) = g_0 + g_1 z^{-1} + g_2 z^{-2} + g_3 z^{-3} + g_4 z^{-4} + \cdots + g_{n_g} z^{-n_g}$$

and

$$n_\mathrm{f} = n_\mathrm{b} - 1, \qquad n_\mathrm{g} = n_\mathrm{a} - 1$$

From (1) and (8) the characteristic polynomial can be derived as:

$$T(z^{-1}) = A(z^{-1})F(z^{-1}) + B(z^{-1})G(z^{-1}) \tag{9}$$

The pole-shifting algorithm makes $T(z^{-1})$ take the form of $A(z^{-1})$ but the pole locations are shifted by a factor α, i.e.

$$A(z^{-1})F(z^{-1}) + B(z^{-1})G(z^{-1}) = A(\alpha z^{-1}) \tag{10}$$

Expanding both sides of (10) and comparing the coefficients gives:

$$\begin{bmatrix} 1 & 0 & \cdots & 0 & b_1 & 0 & \cdots & 0 \\ a_1 & 1 & \cdots & 0 & b_2 & b_1 & \cdots & 0 \\ \vdots & a_1 & \cdots & \vdots & \vdots & b_2 & \cdots & 0 \\ a_{n_a} & \vdots & \cdots & 1 & b_{n_b} & \vdots & \cdots & b_b \\ 0 & a_{n_a} & \cdots & a_1 & 0 & b_{n_b} & \cdots & b_2 \\ \vdots & 0 & \cdots & \vdots & \vdots & 0 & \cdots & \vdots \\ \vdots & \vdots & \cdots & \vdots & \vdots & \vdots & \cdots & \vdots \\ 0 & 0 & \cdots & a_{n_a} & 0 & 0 & \cdots & b_{n_b} \end{bmatrix} \begin{bmatrix} f_1 \\ \vdots \\ \vdots \\ f_{n_f} \\ g_0 \\ \vdots \\ \vdots \\ g_{n_g} \end{bmatrix} = \begin{bmatrix} a_1(\alpha - 1) \\ a_2(\alpha^2 - 1) \\ \vdots \\ \vdots \\ a_{n_a}(\alpha^{n_a} - 1) \\ 0 \\ \vdots \\ 0 \end{bmatrix}$$

or

$$MZ(\alpha) = L(\alpha) \tag{11}$$

If parameters $[\{a_i\}, \{b_i\}]$ are identified at every sampling period, and pole-shift factor α is known, the control parameters $Z = [\{f_i\}, \{g_i\}]$ solved from (11) when substituted in (8) will give:

$$u(t, \alpha) = X^\mathrm{T}(t)Z = X^\mathrm{T}(t)M^{-1}L(\alpha) \tag{12}$$

where

$$X(t) = [\,-u(t-1) \quad -u(t-2)\cdots u(t-n_f) \quad -y(t) - y(t-1) - y(t-2)\cdots y(t-n_g)\,]$$

Expanding the control function in a Taylor series expansion,

$$u(t, \alpha) = u(t, \alpha_o) + \sum_{k=1}^{n_a} s_k \, \Delta\alpha_i^k \tag{13}$$

Considering only a first-order variation, the modification factor $\Delta\alpha$ can be written as:

$$\Delta\alpha = \gamma \left[\frac{\partial u}{\partial \alpha}\right]^{-1} \Delta u \tag{14}$$

where γ is a positive constant chosen to avoid excessive variation of α, and the sensitivity function is computed from (11) as:

$$\frac{\partial u}{\partial \alpha} = X^T M^{-1} \left[\frac{\partial L}{\partial \alpha}\right] = -X^T M^{-1} [\,a_1 \quad 2a_2\alpha \quad 3a_3\alpha^2 \quad \cdots\,]$$

Finally, the variable pole-shift factor $\alpha(t)$ is given as,

$$\alpha(t) = \alpha(t-1) + \Delta\alpha \tag{15}$$

Better estimates of $\Delta\alpha$ can be improved by considering higher order sensitivity terms in (13). The control function is limited by the upper and lower limits and the pole-shift factor should be such that it should be bounded by the reciprocal of the largest value of characteristic root of $A(z^{-1})$. The latter requirement is satisfied by constraining the magnitude of α to unity.

5. The plant model

In the adaptive estimation and control procedure the plant output $y(t)$ is recorded on-line. This measured output is then fed to the estimated plant model to derive the control function.

In the simulation studies however, a plant model is needed to generate $y(t)$. This study considers a fourth-order synchronous machine-exciter given as:

$$\begin{aligned}
\dot{\delta} &= \omega_o \Delta\omega \\
\dot{\omega} &= \frac{1}{2H}[P_m - D\Delta\omega - P_e] \\
\dot{e}'_q &= \frac{1}{T'_{do}}[E_{fd} - e'_{qo} - (x_d - x'_d)i_d] \\
\Delta\dot{E}_{fd} &= \frac{K_A}{T_A}[-\Delta V_t + u_E] - \frac{1}{T_A}\Delta E_{fd}
\end{aligned} \tag{16}$$

The state vector comprises of rotor angle (δ), the generator speed (ω), transient internal voltage (e'_q) and the field voltage (E_{fd}), respectively. The term u_E is the additional control in the excitation system which is considered to be zero in this analysis. The generator power output (P_e), terminal voltage (V_t) are expressed in terms of d–q axes generator currents (i_d, i_q), generator reactances (x_d, x'_d), line impedance, etc. The static VAr compensator circuit, shown in Fig. 2, contains the voltage measuring and the voltage regulator circuits. Normally, the susceptance of the SVC (B) is varied to maintain the mid-bus voltage V_m within its pre-specified tolerance. The variation of the susceptance can be related through the differential equation [10]:

$$\Delta\dot{B} = \frac{-\Delta B + B_o + K_S u}{T_S} \tag{17}$$

K_S and T_S are the gain and time constants, respectively, of the SVC firing angle control circuits, respectively, and u is the input to the thyristor firing angle controller. Combining (17) with the fourth-order generator model, the dynamic equations of the generator-SVC system are expressed as:

$$\dot{x} = f[x, u] \tag{18}$$

This composite dynamic model is solved and the change in the electrical power output P_e is computed at discrete time samples. This is considered to be the output $y(t)$ in this algorithm.

6. Performance with adaptive SVC controller

In order to excite the plant for the identification and control process, a sequence of torque step disturbances are simulated. The diagonal elements of the initial covariance matrix P is assumed be 10,000, the initial pole-shift factor 0.7 and the forgetting factor 1. The starting value of the parameter can be random, but were all considered to be 0.001 in all the simulations for consistency. The model order to be estimated was assumed to be 3. The responses recorded in Figs. 4–8 are for a nominal loading of 0.8 pu at 0.9 pf lagging.

For a sequence of four alternate torque steps of +10%, −10%, +10% and −10%, the speed variation of the generator is shown in Fig. 4. The plant parameters are unknown at the start of the estimation process which gives the poorer response in the early part of the transients. The spikes at 1, 7, 15, 23 s indicate the reversal of torque pulse. Record of electromechanical and electrical transients in Figs. 4 and 5, respectively, exhibit very good transient control by the adaptive strategy.

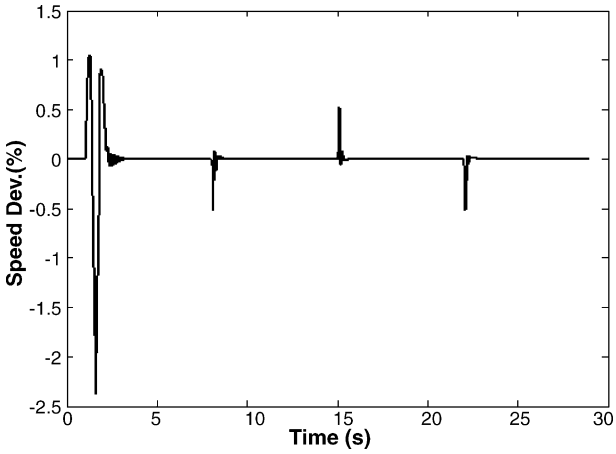

Fig. 4. Generator speed variation with the adaptive identifier-stabilizer subjected to sequences of torque steps.

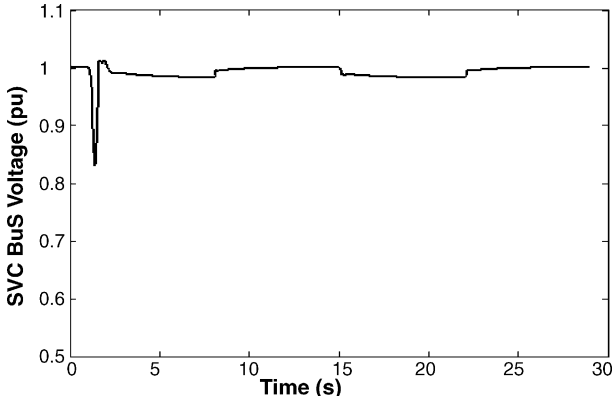

Fig. 5. Variation of SVC bus voltage corresponding to Fig. 4.

The convergence of the $\{a\}$ and $\{b\}$ parameters in the in the adaptive algorithm are shown in Figs. 6 and 7, while Fig. 8 shows the variation of the pole-shift factor as the estimation procedure progressed. The estimation algorithm converges to the desired values rapidly. A good guess as to the value of pole-shift factor can make convergence of the pole-shift factor also faster, as can be seen in Fig. 8.

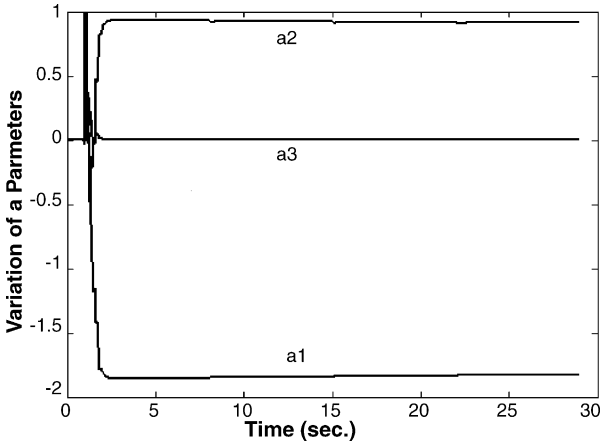

Fig. 6. Variation of 'a' parameters with the progression of the adaptive process.

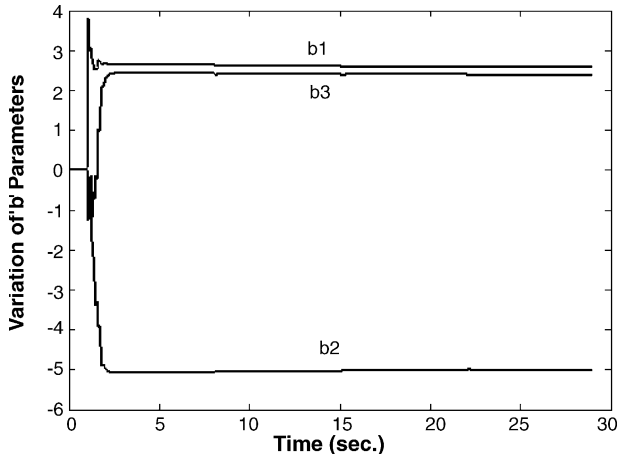

Fig. 7. Variations of '*b*' parameters corresponding to Fig. 6.

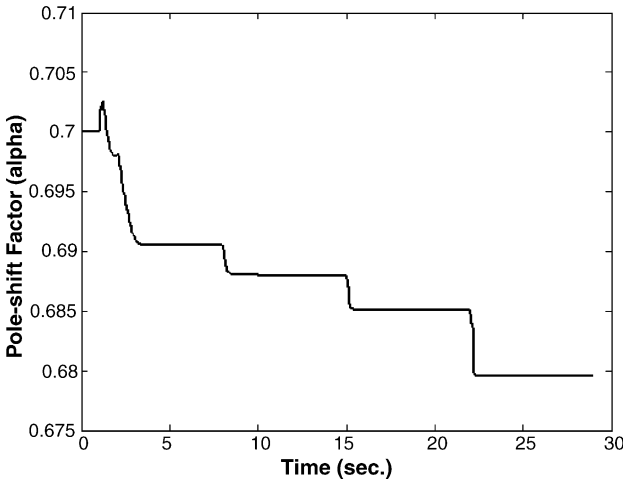

Fig. 8. Variation of the pole-shift factor.

7. Testing the adaptive controller

A number of case studies were performed with the adapted system parameters and the pole-shift parameters arrived at in the previous section. For a 30% input torque pulse on the generator the transients recorded for five operating conditions are shown in Fig. 9. These are generator outputs of (a) 1.2 pu, (b) 1.1 pu, (c) 1 pu, (d) 0.8 pu and (e) 0.5 pu. It can be observed that the damping properties are very good for the whole range of operation considered. It is to be noted that without control the system is under damped, in general, and unstable in some cases. Fig. 10 depicts a comparison of the responses with and without SVC stabilizer when the generator is loaded to 1pu; without control the system is unstable.

Fig. 11 shows the transient angle variations of the generator with the proposed adaptive control strategy for a severe three-phase fault for the five loading conditions considered in Fig. 9. Fig. 12 shows the variations of the SVC bus voltage. For legibility only three cases are shown for the SVC voltage, these are (a) 1.2 pu, (b) 0.8 pu and (c) 0.5 pu loadings. Simulations were carried out with the converged plant model and pole-shift factor as obtained in the nominal loading considered in Figs. 4–8. In real applications, the models as well as the controls will be tuned on-line and is, hence, expected to provide better performance. All these simulation results indicate good dynamic behavior of the power system with the adaptive SVC controller.

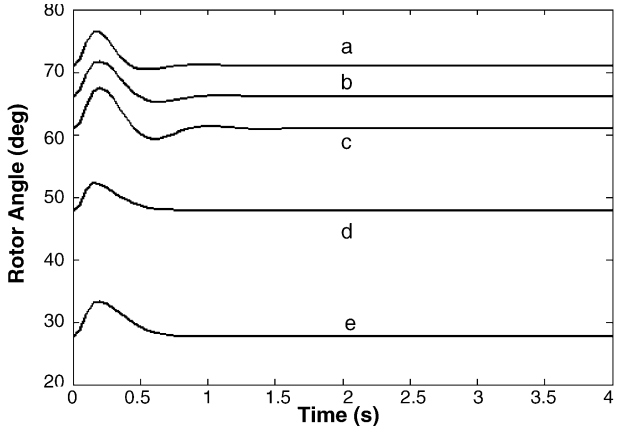

Fig. 9. Generator rotor angle for a 30% torque pulse for 0.1 s for different loadings.

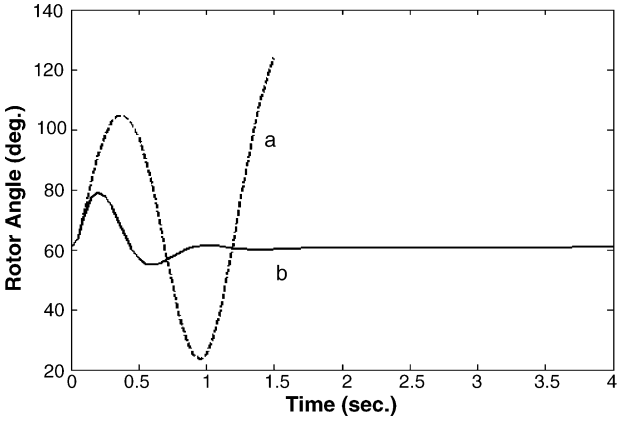

Fig. 10. Rotor angle variations for a three-phase fault of 0.1 s duration for pre-fault load of 1 pu with (a) no control and (b) adaptive strategy.

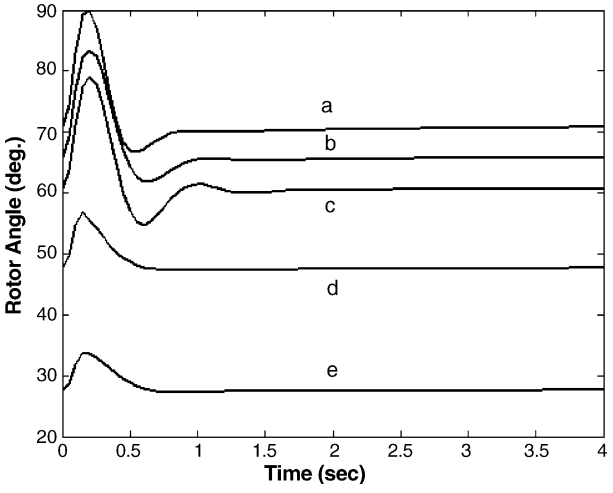

Fig. 11. Rotor angle variations for various loading conditions following a three-phase fault for 0.1 s duration.

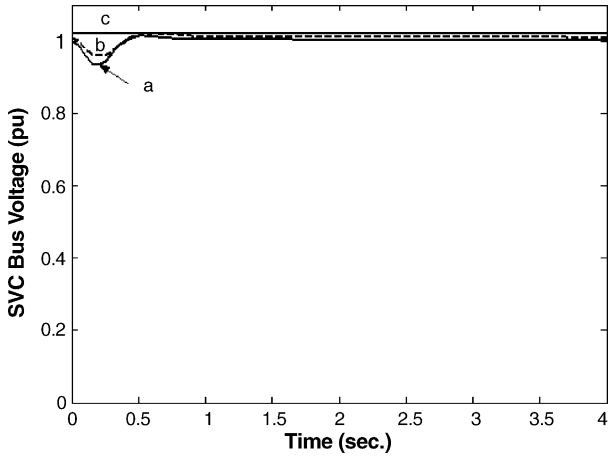

Fig. 12. SVC bus voltage variations with adaptive control corresponding to Fig. 11.

8. Evaluation of the adaptive control strategy

The damping properties of the adaptive self-tuning SVC controller were compared with a conventional PI controller (Fig. 13). The PI controllers are widely used in many power system and other control applications.

The PI or PID controllers are normally installed in the feedback path. An additional washout is included in cascade with the controller to eliminate any unwanted signal in the steady state. The washout time constant (T_w) should be relatively large. The controller function in the feedback loop is written as:

$$H(s) = \left[K_P + \frac{K_I}{s}\right]\left[\frac{sT_w}{1+sT_w}\right] \tag{19}$$

A pole-placement technique was used to determine the optimum gain settings (K_P and K_I) of the controller. For a desired location of the dominant closed-loop eigenvalue λ, the following equation is solved for K_P and K_I,

$$H(\lambda) = [C(\lambda I - A)^{-1}]^{-1} \tag{20}$$

$H(\lambda)$ is obtained from (19) for the desired λ. The dominant eigenvalues of the closed loop system in the present study were selected to be at $-1.9 \pm j6.02$, corresponding to a damping ratio of approximately 0.3. The values for K_P and K_I were found to be −10.5565 and −14.6302, respectively.

Comparison of the responses with the PI control and proposed robust strategies for a three-phase fault for 0.1 s is shown in Figs. 14 and 15. The three loading conditions for the transient rotor angle and SVC-bus voltage variations recorded are for

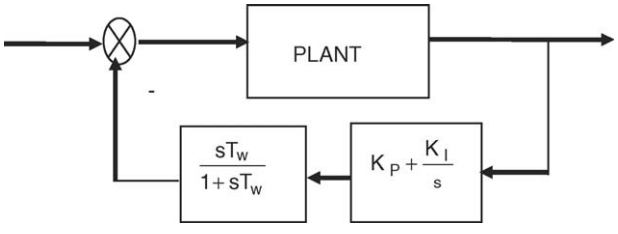

Fig. 13. PI controller block diagram.

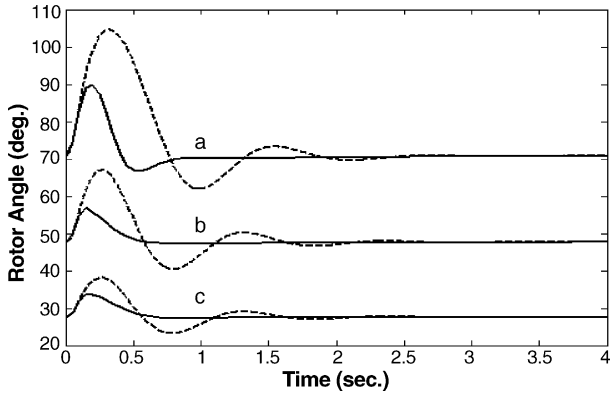

Fig. 14. Comparison of the responses of the adaptive and PI controllers (the dashed lines are with PI controls).

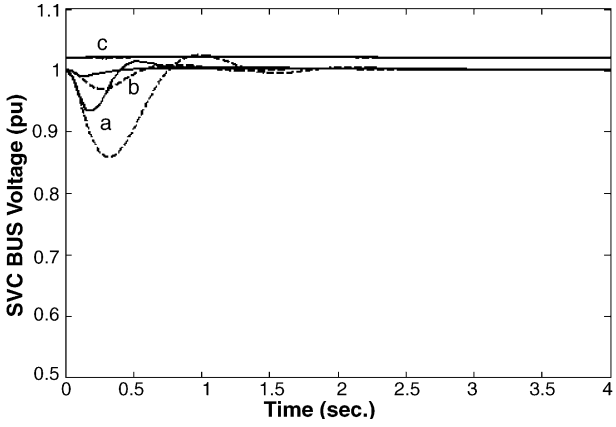

Fig. 15. Mid-bus voltage comparisons corresponding to Fig. 14.

loadings of (a) 1.2 pu, (b) 0.8 pu and (c) 0.5 pu. The solid lines are with the proposed adaptive control and the dashed ones with PI control. While the response with the PI control is reasonably good at operating points closer to the nominal value which it is designed for, they starts to deteriorate as the point of operation moves away. The response with the proposed adaptive controller can be observed to be superior to the 'optimized' PI controller.

9. Conclusions

An adaptive control technique has been used to enhance the dynamic performance of a power system installed with SVC. The proposed stabilizing technique identifies the plant model on-line and generates a control to stabilize the closed-loop system employing a pole-shift technique. The algorithm has been shown to converge to estimated parameter model rapidly. The on-line controller has demonstrated to provide very good damping to the system transients.

The proposed self-tuning adaptive SVC was tested for various disturbances on a number of operating conditions. The stabilizing control was observed to perform robustly over a wide range of operation. Evaluation of the controller through PI controller also demonstrated the superiority of the proposed technique.

Acknowledgement

The authors wish to acknowledge the facilities provided at the King Fahd University of Petroleum & Minerals, Dhahran, Saudi Arabia.

Appendix A

The system data in per unit (except as stated):

$R = 0.01$;
$X = 0.3$;
$g = 0.04$;
$b = -0.38$;
$x'_d = 0.45$;
$x_d = 1.7$;
$x_q = 1.25$;
$H = 4$ s;
$K_A = 4.0$;
$T_A = 0.03$ s;
$K_S = 10$;
$T_S = 0.01$;
$T'_{do} = 6.3\,s$;
$T_w = 1$.

The nominal operating quantities:

$v_t = 1.0$;
$P = 0.8$;
$Q = 0.3874$;
$v_o = 1.0$;
$\delta = 48^\circ$.

References

[1] IEEE Special Stability Controls Working Group, Static VAr compensator models for power flow and dynamic performance simulation, IEEE Trans. Power Syst. 9 (1) (1994) 229–240.
[2] S.H. Hosseini, O. Mirshekhar, Optimal control of SVC for subsynchronous resonance stability in typical power system, Proc. ISIE 2 (2001) 916–921.
[3] S.E.M. Oliveria, Synchronizing and damping torque coefficients and power system steady state stability as affected by static VAr compensators, IEEE Trans. Power Syst. 9 (1) (1994) 109–116.
[4] P.L. So, T. Yu, Coordination of TCSC and SVC for inter area stability enhancement, Proc. POWERCON 1 (2000) 553–558.
[5] Q. Zhao, J. Jiang, Robust SVC controller design for improving power system damping, IEEE Trans. Power Syst. 10 (4) (1995) 1927–1932.
[6] W.M. Hussein, O.P. Malik, Study of system performance with duplicate adaptive power system stabilizer, Electr. Power Components Syst. 31 (2003) 899–912.
[7] A. Soos, O.P. Malik, An H_2 optimal adaptive power system stabilizer, IEEE Trans. Energy Conversion 17 (1) (2002) 143–149.
[8] J.R. Smith, D.A. Pierre, D.A. Rudberg, I. Sadhigi, A.P. Johnson, J.F. Hauer, An enhanced LQ adaptive VAr unit controller for power system damping, IEEE Trans. Power Syst. 4 (2) (1989) 443–451.
[9] P.K. Dash, P.C. Panda, A.M. Sharaf, E.F. Hill, Adaptive controller for static reactive power compensation in power systems, Proc. IEE 134 (3) (1987) 256–284.
[10] M.Z. El-Sadek, G. El-Saady, M. Abo-El-Saud, A variable structure adaptive neural network static VAR controller, Electr. Power Syst. Res. 45 (1998) 109–117.
[11] R. Lozano-Leal, C. Goodwin-Graham, A globally covergent adaptive pole-placement algorithm with persistency of excitation requirements, IEEE Trans. Automatic Control AC 30 (8) (1985) 795–798.
[12] O.P. Malik, G.P. Chen, G.S. Hope, Q.H. Qin, G.Y. Xu, Adaptive self-optimizing pole shifting control algorithm, IEE Proc. D 139 (5) (1992) 429–438.